



Article

Thermal Prediction of Convective-Radiative Porous Fin Heatsink of Functionally Graded Material Using Adomian Decomposition Method

George Oguntala ^{1,*} , Gbeminiyi Sobamowo ², Yinusa Ahmed ² and Raed Abd-Alhameed ¹ 

¹ Department of Biomedical and Electronics Engineering, Faculty of Engineering and Informatics, University of Bradford, West Yorkshire BD7 1DP, UK; r.a.a.abd@bradford.ac.uk

² Department of Mechanical Engineering, Faculty of Engineering, University of Lagos, Akoka, Lagos 100213, Nigeria; mikegbeminiyi@gmail.com (G.S.); aayinusa@unilag.edu.ng (Y.A.)

* Correspondence: g.a.oguntala@bradford.ac.uk

Received: 16 February 2019; Accepted: 20 March 2019; Published: 24 March 2019



Abstract: In recent times, the subject of effective cooling have become an interesting research topic for electronic and mechanical engineers due to the increased miniaturization trend in modern electronic systems. However, fins are useful for cooling various low and high power electronic systems. For improved thermal management of electronic systems, porous fins of functionally graded materials (FGM) have been identified as a viable candidate to enhance cooling. The present study presents an analysis of a convective–radiative porous fin of FGM. For theoretical investigations, the thermal property of the functionally graded material is assumed to follow linear and power-law functions. In this study, we investigated the effects of inhomogeneity index of FGM, convective and radiative variables on the thermal performance of the porous heatsink. The results of the present study show that an increase in the inhomogeneity index of FGM, convective and radiative parameter improves fin efficiency. Moreover, the rate of heat transfer in longitudinal FGM fin increases as β increases. The temperature prediction using the Adomian decomposition method is in excellent agreement with other analytical and method.

Keywords: functionally graded materials; heatsink; porous media; thermal management

1. Introduction

Increased miniaturization in modern consumer electronics has motivated research on thermal management of high-performance microprocessor-based systems by mechanical and electronic designers. High computational performance of electronic systems usually demands increased power and on-chip power density requirements, both of which involve increased heat dissipation. However, to achieve effective cooling of electronic systems, fins are used as passive approach to reduce thermally-induced failures in electronic components. Moreover, porous fins are established to exhibit improved performance over solid fins following the research discovery by Kiwan et al. [1]. Consequently, there are diverse works on the subject of fin using different materials, profiles, orientation and operating conditions in the literature [2–9].

Different works, in recent times, have conducted research using the analytical, numerical and experimental methodology to investigate the effects of various thermal parameters on fin performance [10–16]. Seyf et al. carried out computational analysis of nanofluid effects on convective heat transfer of micro-pin-fin heatsinks [17]. Fazeli et al. experimentally and numerically examined the effect of using silica nanofluid on heat transfer in a miniature heat sink [18]. Other have studied these methodologies to investigate the effects of conventional airflow properties and features of

channel cross-section as an approach to enhance heat transfer via heat sinks. Such studies include Kim and Mudawar which develop analytical heat diffusion models for different microchannel heatsink cross-sectional geometries as a means to investigate heat transfer enhancement [19]. Naphon et al. present a numerical investigation of the convective heat flow and pressure drop in mini-fin and microchannel heat sink for central processing unit cooling [20,21]. Kim and Kim investigate the fluid flow and the characteristics of heat transfer in cross-cut heatsinks [22]. Oguntala et al. present various numerical investigations on the effects of particle deposition, surface roughness, porosity and magnetic field on the thermal performance of porous micro-fin and longitudinal heatsinks [23–25]. Wan et al. [26] present an experimental analysis of flow and heat transfer in a miniature porous heat sink for high heat flux applications. These studies explore the convective, radiative and various thermal parameters of the heatsink using the properties of conventional airflow, features of channel cross-section, variable geometries and air flow paths.

Nevertheless, the use of materials of changing composition, microstructure, or porosity across the material volume has been identified as a reliable candidate for improving the thermal performance of heat sinks. Such inhomogeneous materials of varying physical properties including electrical, chemical, mechanical, magnetic and thermal properties over the volume of the bulk material are referred to as functionally graded material (FGM). The continuous variations in properties in FGM along a specific axis are based on the porosity and pore size, chemical, and microstructural gradient-structures resulting in its increased popularity for various applications including nuclear, automobile structure, aerospace and optoelectronics.

With the thermal capabilities of FGM, its application as heatsink fin would serve as a viable cooling material. However, an in-depth review of existing work shows that research on the application of FGM for heatsink design is not exhaustive in the literature. Therefore, the present work is motivated by the capabilities of FGM and several established thermal characteristics of porous fins. The present work focuses on the analysis of a porous FGM heatsink operating under a convective–radiative environment for improved cooling low and high power electronic systems. The thermal property of FGM is assumed to follow linear and power-law functions. The developed thermal models are solved using Adomian decomposition method (ADM). The approximate analytical solutions are used to study the effects of inhomogeneity index of FGM, convective and radiative parameters on the thermal performance of the porous heat sink.

The paper is organized as follows: the fin problem is formulated in Section 2. A detailed description of ADM used for the nonlinear heat transfer analysis is presented in Section 3. The fin efficiency is presented in Section 4. The developed results of the present study are presented and discussed in Section 5. The conclusions of the study are summarized in Section 6.

2. Formulation of the Model

We consider a porous fin made of FGM as shown in Figure 1. The geometrical dimensions of the fin are given as: length L , width W and thickness t , with both faces of the fin exposed to a convective–radiative environment at temperature T_∞ .

Assume the porous medium is homogeneous, isotropic, and saturated with single-phase fluid and the physical properties of solid as well as fluid are considered as constant. The fluid and porous medium are locally in the thermodynamic domain. The surface radiative transfers and non-Darcian effects are negligible. The temperature variation inside the fin is one-dimensional, that is, temperature varies along the length only and remains constant with time. There is no thermal contact resistance at the fin base and the fin tip is of adiabatic type.

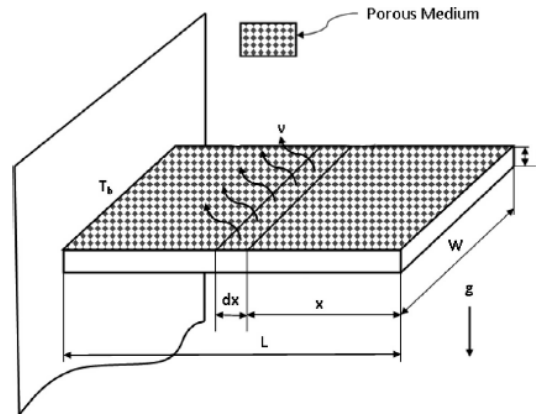


Figure 1. Schematic representation of the fin problem under investigation.

Using the above assumptions, the energy balance of the fin [23] is expressed as:

$$q_x - \left(q_x + \frac{\delta q}{\delta x} dx \right) = \dot{m} c_p (T - T_a) + hP(1 - \tilde{\varepsilon})(T - T_a)dx + \sigma \varepsilon P(T^4 - T_a^4)dx \quad (1)$$

The mass flow rate of the fluid passing through the porous material is expressed as:

$$\dot{m} = \rho u(x) W dx \quad (2)$$

and from the Darcy model

$$u(x) = \frac{g K \beta}{\nu} (T - T_a) \quad (3)$$

Equation (1) becomes

$$q_x - \left(q_x + \frac{\delta q}{\delta x} dx \right) = \frac{\rho c_p g K \beta}{\nu} (T - T_a)^2 dx + hP(1 - \tilde{\varepsilon})(T - T_a)dx + \sigma \varepsilon P(T^4 - T_a^4)dx \quad (4)$$

However, as $dx \rightarrow 0$, Equation (4) reduces to

$$-\frac{dq}{dx} = \frac{\rho c_p g K \beta}{\nu} (T - T_a)^2 + hP(1 - \tilde{\varepsilon})(T - T_a) + \sigma \varepsilon P(T^4 - T_a^4) \quad (5)$$

From Fourier's law of heat conduction, the heat flow in the fin with FGM is expressed as:

$$q = -k_{eff}(x) A_{cr} \frac{dT}{dx} \quad (6)$$

where

$$k_{eff}(x) = \phi k_f + (1 - \phi) k_s \quad (7)$$

$$\frac{d}{dx} \left(k_{eff}(x) A_{cr} \frac{dT}{dx} \right) = \frac{\rho c_p g K \beta}{\nu} (T - T_a)^2 + hP(1 - \tilde{\varepsilon})(T - T_a) + \sigma \varepsilon P(T^4 - T_a^4) \quad (8)$$

simplifying Equation (8) gives the governing differential equation of the fin as:

$$\frac{d}{dx} \left(k_{eff}(x) \frac{dT}{dx} \right) - \frac{\rho c_p g K \beta}{t \nu} (T - T_a)^2 - \frac{h(1 - \tilde{\varepsilon})}{t} (T - T_a) - \frac{\sigma \varepsilon}{t} (T^4 - T_a^4) \quad (9)$$

The boundary conditions are

$$\begin{aligned} x = 0, \frac{dT}{dx} &= 0 \\ x = L, T &= T_b \end{aligned} \quad (10)$$

When the Temperature Difference in the Fin is Small during Heat Flow

The scenario considered in this section is one where a small temperature difference exists within the material during the heat flow. Such condition necessitates the use of temperature-invariant physical and thermal properties of the fin. Moreover, under such condition, it is established that the term T^4 can be expressed as a linear function of temperature [27]. Therefore, we have;

$$T^4 = T_\infty^4 + 4T_\infty^3(T - T_\infty) + 6T_\infty^2(T - T_\infty)^2 + \dots \cong 4T_\infty^3 T - 3T_\infty^4 \quad (11)$$

On substituting Equation (11) into Equation (9), we arrived at

$$\frac{d}{dx} \left(k_{eff}(x) \frac{dT}{dx} \right) - \frac{\rho c_p g K \beta}{tv} (T - T_a)^2 - \frac{h(1 - \tilde{\epsilon})}{t} (T - T_a) - \frac{4\sigma \epsilon P T_a^3}{t} (T - T_a) = 0 \quad (12)$$

For the FGM fin, the spatial-dependent thermal conductivities is established [28] as follows:
Exponential-law function

$$k_{eff}(x) = k_o \exp^{\alpha(1 - (\frac{x}{L}))} \quad (13)$$

Power-law function

$$k_{eff} = k_o \left(\frac{x}{L} \right)^{-\beta} \quad (14)$$

where $\alpha < 0$ and $\beta > 0$.

On substituting the following dimensionless parameters in Equation (15) into Equations (12)–(14)

$$X = \frac{x}{L}, \theta = \frac{T - T_a}{T_b - T_a}, Ra = \frac{gk\beta(T_b - T_\infty)b}{\alpha\nu k_r}, Nc = \frac{pbh}{A_b k_{eff}}, Rd = \frac{4\sigma T_\infty^3}{3\beta_R k_{eff}}, Nr = \frac{4\sigma b T_\infty^3}{k_{eff}}, \quad (15)$$

$$H = \frac{\sigma_m B_0^2 u^2}{k_{eff} A_b}, N^2 = \frac{q_o''' b^2}{k_{eff}(T_b - T_a)}, C_T = \frac{T_\infty}{T_b - T_\infty}$$

The dimensionless forms of the governing equation in Equation (12) is expressed as:
Exponential law function

$$\frac{d}{dX} \left[e^{\alpha(1-X)} \frac{d\theta}{dX} \right] - Ra\theta^2 - Nc(1 - \tilde{\epsilon})\theta - Nr\theta = 0 \quad (16)$$

Power-law function

$$\frac{d}{dX} \left[\left(X^{-\beta} \right) \frac{d\theta}{dX} \right] - Ra\theta^2 - Nc(1 - \tilde{\epsilon})\theta - Nr\theta = 0 \quad (17)$$

on expanding Equations (16) and (17), we obtain

Exponential law function

$$e^{-\alpha X} \frac{d^2\theta}{dX^2} - \alpha e^{-\alpha X} \frac{d\theta}{dX} - e^{-\alpha} (Ra\theta^2 + Nc(1 - \tilde{\epsilon})\theta + Nr\theta) = 0 \quad (18)$$

Power-law function

$$X^{-\beta} \frac{d^2\theta}{dX^2} - \beta X^{-\beta-1} \frac{d\theta}{dX} - Ra\theta^2 - Nc(1 - \tilde{\epsilon})\theta - Nr\theta = 0 \quad (19)$$

and the dimensionless boundary conditions are

$$X = 0, \frac{d\theta}{dX} = 0 \quad (20a)$$

$$X = 1, \theta = 1 \quad (20b)$$

For a solid fin, i.e., the non-porous fin of FGM, the governing differential equations are

Exponential law function

$$e^{-\alpha X} \frac{d^2 \theta}{dX^2} - \alpha e^{-\alpha X} \frac{d\theta}{dX} - e^{-\alpha} (Nc(1 - \tilde{\varepsilon}) + Nr) \theta = 0 \quad (21)$$

Power-law function

$$X^{-\beta} \frac{d^2 \theta}{dX^2} - \beta X^{-\beta-1} \frac{d\theta}{dX} - (Nc(1 - \tilde{\varepsilon}) + Nr) \theta = 0 \quad (22)$$

An approximate analytical solution can easily be developed using Bessel function and mean-value theorem such that Equations (21) and (22) becomes:

Exponential-law function

$$\theta(X) = \frac{e^{\frac{\alpha(X-1)}{2}} \left\{ K_0 \left(\frac{2}{\beta} \sqrt{(Nc^2 + Nr + Ma^2)} \right) I_1 \left(\frac{2}{\beta} \sqrt{(Nc^2 + Nr + Ma^2)} e^{\frac{\alpha X}{2}} \right) + I_0 \left(\frac{2}{\beta} \sqrt{(Nc^2 + Nr + Ma^2)} \right) K_1 \left(\frac{2}{\beta} \sqrt{(Nc^2 + Nr + Ma^2)} e^{\frac{\alpha X}{2}} \right) \right\}}{\left\{ K_0 \left(\frac{2}{\beta} \sqrt{(Nc^2 + Nr + Ma^2)} \right) I_1 \left(\frac{2}{\beta} \sqrt{(Nc^2 + Nr + Ma^2)} \right) e^{\frac{\alpha}{2}} + I_0 \left(\frac{2}{\beta} \sqrt{(Nc^2 + Nr + Ma^2)} \right) K_1 \left(\frac{2}{\beta} \sqrt{(Nc^2 + Nr + Ma^2)} \right) e^{\frac{\alpha}{2}} \right\}} \quad (23)$$

Power-law function

$$\theta(X) = \frac{\left\{ \left\{ \frac{-\beta(\frac{1}{2})^{-\beta-1} + \sqrt{[\beta(\frac{1}{2})^{-\beta-1}]^2 + 4(Nc^2 + Nr)(\frac{1}{2})^{-\beta}}}{2(\frac{1}{2})^{-\beta}} \exp \left\{ \frac{-\beta(\frac{1}{2})^{-\beta-1} + \sqrt{[\beta(\frac{1}{2})^{-\beta-1}]^2 + 4(Nc^2 + Nr)(\frac{1}{2})^{-\beta}}}{2(\frac{1}{2})^{-\beta}} \right\} + \frac{-\beta(\frac{1}{2})^{-\beta-1} - \sqrt{[\beta(\frac{1}{2})^{-\beta-1}]^2 + 4(Nc^2 + Nr)(\frac{1}{2})^{-\beta}}}{2(\frac{1}{2})^{-\beta}} (1-X) \right\} \right\}}{\left\{ \left\{ \frac{-\beta(\frac{1}{2})^{-\beta-1} + \sqrt{[\beta(\frac{1}{2})^{-\beta-1}]^2 + 4(Nc^2 + Nr)(\frac{1}{2})^{-\beta}}}{2(\frac{1}{2})^{-\beta}} \exp \left\{ \frac{-\beta(\frac{1}{2})^{-\beta-1} + \sqrt{[\beta(\frac{1}{2})^{-\beta-1}]^2 + 4(Nc^2 + Nr)(\frac{1}{2})^{-\beta}}}{2(\frac{1}{2})^{-\beta}} \right\} + \frac{-\beta(\frac{1}{2})^{-\beta-1} - \sqrt{[\beta(\frac{1}{2})^{-\beta-1}]^2 + 4(Nc^2 + Nr)(\frac{1}{2})^{-\beta}}}{2(\frac{1}{2})^{-\beta}} (1-X) \right\} \right\}} \quad (24)$$

It should be noted that the first and second kinds of Bessel and modified Bessel functions are expressed as:

$$\begin{aligned} Y_\nu(z) &= \frac{2}{\pi} \left(\sum_{r=0}^{\infty} \frac{(-1)^r \left(\frac{z}{2}\right)^{2r+\nu}}{r! \Gamma(\nu+r+1)} \right) \ln\left(\frac{z}{2}\right) - \frac{1}{\pi} \sum_{r=0}^{\infty} \frac{(v-r-1)! \left(\frac{z}{2}\right)^{2r-\nu}}{r!} - \frac{1}{\pi} \sum_{r=0}^{\infty} \frac{(-1)^r \left(\frac{z}{2}\right)^{2r+n}}{r! (r+n)!} [\psi(r+\nu+1) + \psi(r+1)], \\ I_\nu(z) &= \sum_{r=0}^{\infty} \frac{\left(\frac{z}{2}\right)^{2r+\nu}}{r! \Gamma(\nu+r+1)}, \\ K_\nu(z) &= (-1)^{\nu+1} \left(\sum_{r=0}^{\infty} \frac{\left(\frac{z}{2}\right)^{2r+\nu}}{r! \Gamma(\nu+r+1)} \right) \ln\left(\frac{z}{2}\right) + \frac{1}{2} \sum_{r=0}^{\infty} \frac{(v-r-1)! \left(\frac{z}{2}\right)^{2r-\nu}}{r!} + \frac{1}{2} (-1)^\nu \sum_{r=0}^{\infty} \frac{(-1)^r \left(\frac{z}{2}\right)^{2r+n}}{r! (r+n)!} [\psi(r+\nu+1) + \psi(r+1)], \end{aligned} \quad (25)$$

3. Analysis of Nonlinear Heat Transfer Equation Using the Adomian Decomposition Method

The nonlinearity in the governing Equations (18) and (19) poses a computational challenge in developing a closed-form solution of the nonlinear heat transfer equations. However, the application of approximate analytical methods such as Adomian decomposition method (ADM) is efficient to overcome such computational challenge. The section discusses the ADM, which is used to solve the developed thermal model.

Principle of ADM

The analytical solutions obtained in Equations (23) and (24) are closed-form solutions of the linearized form of the nonlinear model of the present study. However, when the nonlinear term is incorporated, the developed analytical scheme (special functions) fails. This necessitates the need for an alternative analytical scheme as the numerical approach is employed for verification. ADM is employed in the present study because it transforms only the nonlinear terms into an Adomian function with all the linear terms preserved which increases the accuracy of the method. However,

a strong limitation of ADM is the ability to obtain the right Adomian level, which when obtained, speeds up the convergence of the required solution.

To discuss the principle of ADM, we express its general nonlinear equation in the form:

$$Lu + Ru + Nu = g \quad (26)$$

In Equation (26), the linear terms are decomposed into $L + R$, with L taken as the highest-order derivative that is easily invertible and R as remainder of the linear operator of less derivative order than L . In addition, g represents the source term, u is the system output and Nu represents the nonlinear terms, which is assumed to be analytic. L^{-1} is the inverse operator of L and is defined by a definite integration from 0 to x , i.e.,

$$[L^{-1}f](x) = \int_0^x f(x)dx \quad (27)$$

If L is a second-order operator, then L^{-1} is a two-fold indefinite integral i.e., L^{-1} could be expressed as:

$$[L^{-1}f](x) = \int_0^x \int_0^x f(x)dx dx \quad (28)$$

By applying the inverse operator L^{-1} to both sides of Equation (26), and using the given conditions, the resulting equation is expressed as:

$$u = \mu(x) - L^{-1}Ru - L^{-1}Nu \quad (29)$$

where $\mu(x) = \lambda_x + L^{-1}g$ and λ_x are terms arising from integrating the source term $g(x)$.

The Adomian method decomposes the solution $u(x)$ of Equation (29) into a series form as:

$$u = \sum_{m=0}^{\infty} u_m \quad (30)$$

and the nonlinear term as

$$Nu = \sum_{m=0}^{\infty} A_m \quad (31)$$

where A_m 's are Adomian's polynomials of u_0, u_1, \dots, u_m and are obtained for the nonlinearity $Nu = f(u)$ from the recursive formula

$$A_m = \frac{1}{m!} \left[\frac{d^m}{d\zeta^m} [fu(\zeta)] \right]_{\zeta=0} = \frac{1}{m!} \left[\frac{d^m}{d\zeta^m} f \left(\sum_{i=0}^{\infty} \zeta^i y_i \right) \right]_{\zeta=0} \quad m = 0, 1, 2, 3, \dots \quad (32)$$

where ζ is a grouping parameter of convenience.

The ADM defines the solution of the function $f(x)$ to be approximated as:

$$f(x) = \sum_{m=0}^{\infty} f_m(x) \quad (33)$$

by applying ADM to Equations (18) and (19), we obtain

Exponential law function

$$\frac{d^2\theta}{dX^2} = e^{-\alpha} e^{\alpha X} \left(Ra\theta^2 + Nc(1 - \tilde{\epsilon})\theta + Nr\theta \right) + \alpha \frac{d\theta}{dX} \quad (34)$$

Power-law function

$$\frac{d^2\theta}{dX^2} = \beta X^{-1} \frac{d\theta}{dX} + X^{\beta} \left(Ra\theta^2 + Nc(1 - \tilde{\epsilon})\theta + Nr\theta \right) \quad (35)$$

However, the differential forms of Equations (34) and (35) is expressed as:
Exponential law function

$$L_X \theta = e^{-\alpha} e^{\alpha X} \left(Ra \theta^2 + Nc(1 - \tilde{\varepsilon}) \theta + Nr \theta \right) + \alpha \frac{d\theta}{dX} \quad (36)$$

Power-law function

$$L_X \theta = \beta X^{-1} \frac{d\theta}{dX} + X^\beta Ra \theta^2 + X^\beta Nc(1 - \tilde{\varepsilon}) \theta + X^\beta Nr \theta \quad (37)$$

where $L_X = \frac{d^2}{dX^2}$ is the linear second-order differential operator that is invertible.

On applying the inverse operator, L_X^{-1} on both sides of Equations (36) and (37), we obtain:

Exponential law function

$$\theta(X) = \theta(0) + e^{-\alpha} Ra L_X^{-1} \left(e^{\alpha X} \theta^2 \right) + e^{-\alpha} Nc(1 - \tilde{\varepsilon}) L_X^{-1} \left(e^{\alpha X} \theta \right) + e^{-\alpha} Nr L_X^{-1} \left(e^{\alpha X} \theta \right) + \alpha L_X^{-1} \left(\frac{d\theta}{dX} \right) \quad (38)$$

Power-law function

$$\theta(X) = \theta(0) + \beta L_X^{-1} \left(X^{-1} \frac{d\theta}{dX} \right) + Ra L_X^{-1} \left(X^\beta \theta^2 \right) + Nc(1 - \tilde{\varepsilon}) L_X^{-1} \left(X^\beta \theta \right) + Nr L_X^{-1} \left(X^\beta \theta \right) \quad (39)$$

where $L_X^{-1} = \int_0^X \int_0^X (\bullet) dX dX$ and $\theta(0)$ is the dimensionless tip temperature of the fin, which is denoted as θ_0 .

The unknown θ_m , $m \geq 1$ is decomposed into a sum of components defined by the decomposition series as $\theta = \sum_{m=1}^{\infty} \theta_m$.

Therefore Equations (38) and (39) becomes:

Exponential law function

$$\sum_{m=1}^{\infty} \theta_m = \theta_0 + e^{-\alpha} Ra L_X^{-1} \left(e^{\alpha X} \sum_{m=1}^{\infty} A_m \right) + e^{-\alpha} Nc(1 - \tilde{\varepsilon}) L_X^{-1} \left(e^{\alpha X} \sum_{m=1}^{\infty} \theta_m \right) + e^{-\alpha} Nr L_X^{-1} \left(e^{\alpha X} \sum_{m=1}^{\infty} \theta_m \right) + \alpha L_X^{-1} \left(\sum_{m=1}^{\infty} \frac{d\theta_m}{dX} \right) \quad (40)$$

Power-law function

$$\theta(X) = \theta_0 + \beta L_X^{-1} \left(X^{-1} \sum_{m=1}^{\infty} \frac{d\theta_m}{dX} \right) + Ra L_X^{-1} \left(X^\beta \sum_{m=1}^{\infty} A_m \right) + Nc(1 - \tilde{\varepsilon}) L_X^{-1} \left(X^\beta \sum_{m=1}^{\infty} \theta_m \right) + Nr L_X^{-1} \left(X^\beta \sum_{m=1}^{\infty} \theta_m \right) \quad (41)$$

To determine the higher order terms, Equations (40) and (41) can be written as with a recursive relationship as:

Exponential law function

$$\theta_m = \theta_0 + e^{-\alpha} Ra L_X^{-1} \left(e^{\alpha X} A_{m-1} \right) + e^{-\alpha} Nc(1 - \tilde{\varepsilon}) L_X^{-1} \left(e^{\alpha X} \theta_{m-1} \right) + e^{-\alpha} Nr L_X^{-1} \left(e^{\alpha X} \theta_{m-1} \right) + \alpha L_X^{-1} \left(\frac{d\theta_{m-1}}{dX} \right) \quad (42)$$

where $m \geq 1$.

Power-law function

$$\theta(X) = \theta_0 + \beta L_X^{-1} \left(X^{-1} \frac{d\theta_{m-1}}{dX} \right) + Ra L_X^{-1} \left(X^\beta A_{m-1} \right) + Nc(1 - \tilde{\varepsilon}) L_X^{-1} \left(X^\beta \theta_{m-1} \right) + Nr L_X^{-1} \left(X^\beta \theta_{m-1} \right) \quad (43)$$

Here, the Adomian polynomials for the nonlinear terms are given as follows

$$\begin{aligned} A_0 &= F(\theta_0) \\ A_1 &= \theta_1 F'(\theta_0) \\ A_2 &= \theta_2 F'(\theta_0) + \frac{1}{2} \theta_1^2 F''(\theta_0) \\ A_3 &= \theta_3 F'(\theta_0) + \theta_1 \theta_2 F''(\theta_0) + \frac{1}{6} \theta_1^3 F'''(\theta_0) \end{aligned} \quad (44)$$

$$\begin{aligned}
 A_0 &= \theta_0^2 \\
 A_1 &= 2\theta_0\theta_1 \\
 A_2 &= 2\theta_0\theta_2 + \theta_1^2 \\
 A_3 &= 2\theta_0\theta_3 + 2\theta_1\theta_2 \\
 &\vdots \\
 &\dots
 \end{aligned}
 \tag{45}$$

using the Adomian decomposition scheme in Equation (45) and considering 15 Adomian terms for the nonlinear part of the model, the approximate analytical solution for the exponential law is expressed as:

$$\begin{aligned}
 \theta(X) = & \theta_0 + \frac{\theta_0[\theta_0 Ra + (Nc(1-\tilde{\epsilon}) + Nr)]}{4\alpha^4} (4e^{\alpha X} - \alpha^2 X^2 - 4\alpha X - 4) \\
 & + \frac{\theta_0[\theta_0 Ra + (Nc(1-\tilde{\epsilon}) + Nr)]}{4\alpha^4} [2\theta_0 Ra + (Nc(1-\tilde{\epsilon}) + Nr)] (e^{2\alpha X} - 4\alpha X e^{\alpha X} + 4e^{\alpha X} - 2\alpha X - 5) \\
 & + \frac{\theta_0[\theta_0 Ra + (Nc(1-\tilde{\epsilon}) + Nr)]}{36\alpha^6} \left\{ \begin{aligned} & [2\theta_0 Ra + (Nc(1-\tilde{\epsilon}) + Nr)]^2 \\ & + 4\theta_0 Ra [\theta_0 Ra + (Nc(1-\tilde{\epsilon}) + Nr)] \end{aligned} \right\} (e^{3\alpha X} - 3\alpha X - 1) \\
 & - \frac{\theta_0[\theta_0 Ra + (Nc(1-\tilde{\epsilon}) + Nr)]}{4\alpha^6} \left\{ \begin{aligned} & [\theta_0 Ra + (Nc(1-\tilde{\epsilon}) + Nr)]^2 \\ & + 2\theta_0 Ra [\theta_0 Ra + (Nc(1-\tilde{\epsilon}) + Nr)] \end{aligned} \right\} (aX e^{2\alpha X} - e^{2\alpha X} + \alpha X + 1) \\
 & + \frac{\theta_0[\theta_0 Ra + (Nc(1-\tilde{\epsilon}) + Nr)]}{8\alpha^6} \left\{ \begin{aligned} & [2\theta_0 Ra + (Nc(1-\tilde{\epsilon}) + Nr)]^2 \\ & - 4\theta_0 Ra [\theta_0 Ra + (Nc(1-\tilde{\epsilon}) + Nr)] \end{aligned} \right\} (e^{2\alpha X} - 2\alpha X - 1) \\
 & - \frac{\theta_0[\theta_0 Ra + (Nc(1-\tilde{\epsilon}) + Nr)]}{2\alpha^6} \left\{ \begin{aligned} & [\theta_0 Ra + (Nc(1-\tilde{\epsilon}) + Nr)]^2 \\ & - 4\theta_0 Ra [\theta_0 Ra + (Nc(1-\tilde{\epsilon}) + Nr)] \end{aligned} \right\} (aX e^{2\alpha X} - 2e^{2\alpha X} + \alpha X + 2) \\
 & + \frac{\theta_0[\theta_0 Ra + (Nc(1-\tilde{\epsilon}) + Nr)]}{4\alpha^6} \left\{ \begin{aligned} & 4\theta_0 Ra [\theta_0 Ra + (Nc(1-\tilde{\epsilon}) + Nr)] \\ & - [2\theta_0 Ra + (Nc(1-\tilde{\epsilon}) + Nr)]^2 \end{aligned} \right\} (e^{\alpha X} - \alpha X - 1) \\
 & + \frac{\theta_0 Ra [\theta_0 Ra + (Nc(1-\tilde{\epsilon}) + Nr)]^2}{\alpha^6} (a^2 X^2 e^{\alpha X} - 4X e^{\alpha X} + 6e^{\alpha X} - 2\alpha X - 6) + \dots
 \end{aligned}
 \tag{46}$$

Moreover, we show that the solution for the power-law for $\beta = -1/2$ is:

$$\begin{aligned}
 \theta(X) = & \theta_0 + 4\theta_0[\theta_0 Ra + (Nc(1-\tilde{\epsilon}) + Nr)] \frac{X^{3/2}}{3!} \\
 & + 64\theta_0[\theta_0 Ra + (Nc(1-\tilde{\epsilon}) + Nr)] [2\theta_0 Ra + (Nc(1-\tilde{\epsilon}) + Nr)] \frac{X^3}{6!} \\
 & + 256\theta_0[\theta_0 Ra + (Nc(1-\tilde{\epsilon}) + Nr)] \left\{ \begin{aligned} & 7[2\theta_0 Ra + (Nc(1-\tilde{\epsilon}) + Nr)]^2 \\ & + 5\theta_0 Ra [\theta_0 Ra + (Nc(1-\tilde{\epsilon}) + Nr)] \end{aligned} \right\} \frac{X^{9/2}}{9!} \\
 & + 2048 \left\{ \begin{aligned} & \theta_0[\theta_0 Ra + (Nc(1-\tilde{\epsilon}) + Nr)] [2\theta_0 Ra + (Nc(1-\tilde{\epsilon}) + Nr)] \\ & \cdot \left\{ 35[2\theta_0 Ra + (Nc(1-\tilde{\epsilon}) + Nr)]^2 + 109\theta_0 Ra [\theta_0 Ra + (Nc(1-\tilde{\epsilon}) + Nr)] \right\} \end{aligned} \right\} \frac{X^6}{12!} + \dots
 \end{aligned}
 \tag{47}$$

It is worth noting that for homogenous porous fin, $\beta = 0$.

$$\begin{aligned}
 \theta(X) = & \theta_0 + \theta_0[\theta_0 Ra + (Nc(1-\tilde{\epsilon}) + Nr)] \frac{X^2}{2!} \\
 & + \theta_0[\theta_0 Ra + (Nc(1-\tilde{\epsilon}) + Nr)] [2\theta_0 Ra + (Nc(1-\tilde{\epsilon}) + Nr)] \frac{X^4}{4!} \\
 & + [\theta_0 Ra + (Nc(1-\tilde{\epsilon}) + Nr)] \left\{ \begin{aligned} & [2\theta_0 Ra + (Nc(1-\tilde{\epsilon}) + Nr)]^2 \\ & + 6\theta_0 Ra [\theta_0 Ra + (Nc(1-\tilde{\epsilon}) + Nr)] \end{aligned} \right\} \frac{X^6}{6!} \\
 & + \left\{ \begin{aligned} & \theta_0[\theta_0 Ra + (Nc(1-\tilde{\epsilon}) + Nr)] [2\theta_0 Ra + (Nc(1-\tilde{\epsilon}) + Nr)] \\ & \cdot \left\{ [2\theta_0 Ra + (Nc(1-\tilde{\epsilon}) + Nr)]^2 + 6\theta_0 Ra [\theta_0 Ra + (Nc(1-\tilde{\epsilon}) + Nr)] \right\} \end{aligned} \right\} \frac{X^8}{8!} + \dots
 \end{aligned}
 \tag{48}$$

θ_0 is the unknown dimensionless tip temperature of the fin, which can be determined by applying Equation (20b).

$$\begin{aligned}
 1 = & \theta_0 + 4\theta_0[\theta_0 Ra + (Nc(1-\tilde{\epsilon}) + Nr)] \frac{1}{3!} \\
 & + 64\theta_0[\theta_0 Ra + (Nc(1-\tilde{\epsilon}) + Nr)] [2\theta_0 Ra + (Nc(1-\tilde{\epsilon}) + Nr)] \frac{1}{6!} \\
 & + 256\theta_0[\theta_0 Ra + (Nc(1-\tilde{\epsilon}) + Nr)] \left\{ \begin{aligned} & 7[2\theta_0 Ra + (Nc(1-\tilde{\epsilon}) + Nr)]^2 \\ & + 5\theta_0 Ra [\theta_0 Ra + (Nc(1-\tilde{\epsilon}) + Nr)] \end{aligned} \right\} \frac{1}{9!} \\
 & + 2048 \left\{ \begin{aligned} & \theta_0[\theta_0 Ra + (Nc(1-\tilde{\epsilon}) + Nr)] [2\theta_0 Ra + (Nc(1-\tilde{\epsilon}) + Nr)] \\ & \cdot \left\{ 35[2\theta_0 Ra + (Nc(1-\tilde{\epsilon}) + Nr)]^2 + 109\theta_0 Ra [\theta_0 Ra + (Nc(1-\tilde{\epsilon}) + Nr)] \right\} \end{aligned} \right\} \frac{1}{12!} + \dots
 \end{aligned}
 \tag{49}$$

The exponential law in Equation (46) becomes

$$\begin{aligned}
 1 = \theta_0 + & \frac{\theta_0[\theta_0 Ra + (Nc(1-\tilde{\epsilon}) + Nr)]}{2\alpha^2} (4e^\alpha - \alpha^2 - 4\alpha - 4) \\
 & + \frac{\theta_0[\theta_0 Ra + (Nc(1-\tilde{\epsilon}) + Nr)]}{4\alpha^4} [2\theta_0 Ra + (Nc(1-\tilde{\epsilon}) + Nr)] (e^{2\alpha} - 4\alpha e^\alpha + 4e^\alpha - 2\alpha - 5) \\
 & + \frac{\theta_0[\theta_0 Ra + (Nc(1-\tilde{\epsilon}) + Nr)]}{36\alpha^6} \left\{ \begin{aligned} & [2\theta_0 Ra + (Nc(1-\tilde{\epsilon}) + Nr)]^2 \\ & + 4\theta_0 Ra[\theta_0 Ra + (Nc(1-\tilde{\epsilon}) + Nr)] \end{aligned} \right\} (e^{3\alpha} - 3\alpha - 1) \\
 & - \frac{\theta_0[\theta_0 Ra + (Nc(1-\tilde{\epsilon}) + Nr)]}{4\alpha^6} \left\{ \begin{aligned} & [\theta_0 Ra + (Nc(1-\tilde{\epsilon}) + Nr)]^2 \\ & + 2\theta_0 Ra[\theta_0 Ra + (Nc(1-\tilde{\epsilon}) + Nr)] \end{aligned} \right\} (ae^{2\alpha} - e^{2\alpha} + \alpha + 1) \\
 & + \frac{\theta_0[\theta_0 Ra + (Nc(1-\tilde{\epsilon}) + Nr)]}{8\alpha^6} \left\{ \begin{aligned} & [2\theta_0 Ra + (Nc(1-\tilde{\epsilon}) + Nr)]^2 \\ & - 4\theta_0 Ra[\theta_0 Ra + (Nc(1-\tilde{\epsilon}) + Nr)] \end{aligned} \right\} (e^{2\alpha} - 2\alpha - 1) \\
 & - \frac{\theta_0[\theta_0 Ra + (Nc(1-\tilde{\epsilon}) + Nr)]}{2\alpha^6} \left\{ \begin{aligned} & [\theta_0 Ra + (Nc(1-\tilde{\epsilon}) + Nr)]^2 \\ & - 4\theta_0 Ra[\theta_0 Ra + (Nc(1-\tilde{\epsilon}) + Nr)] \end{aligned} \right\} (ae^{2\alpha} - 2e^{2\alpha} + \alpha + 2) \\
 & + \frac{\theta_0[\theta_0 Ra + (Nc(1-\tilde{\epsilon}) + Nr)]}{4\alpha^6} \left\{ \begin{aligned} & 4\theta_0 Ra[\theta_0 Ra + (Nc(1-\tilde{\epsilon}) + Nr)] \\ & - [2\theta_0 Ra + (Nc(1-\tilde{\epsilon}) + Nr)]^2 \end{aligned} \right\} (e^\alpha - \alpha - 1) \\
 & + \frac{\theta_0 Ra[\theta_0 Ra + (Nc(1-\tilde{\epsilon}) + Nr)]^2}{\alpha^6} (a^2 e^\alpha - 4e^\alpha + 6e^\alpha - 2\alpha - 6) + \dots
 \end{aligned} \quad (50)$$

while the homogenous porous fin where $\beta = 0$.

$$\begin{aligned}
 \theta(X) = & \theta_0 + \theta_0[\theta_0 Ra + (Nc(1-\tilde{\epsilon}) + Nr)] \frac{X^2}{2!} \\
 & + \theta_0[\theta_0 Ra + (Nc(1-\tilde{\epsilon}) + Nr)] [2\theta_0 Ra + (Nc(1-\tilde{\epsilon}) + Nr)] \frac{X^4}{4!} \\
 & + [\theta_0 Ra + (Nc(1-\tilde{\epsilon}) + Nr)] \left\{ \begin{aligned} & [2\theta_0 Ra + (Nc(1-\tilde{\epsilon}) + Nr)]^2 \\ & + 6\theta_0 Ra[\theta_0 Ra + (Nc(1-\tilde{\epsilon}) + Nr)] \end{aligned} \right\} \frac{X^6}{6!} \\
 & + \left\{ \begin{aligned} & \theta_0[\theta_0 Ra + (Nc(1-\tilde{\epsilon}) + Nr)] [2\theta_0 Ra + (Nc(1-\tilde{\epsilon}) + Nr)] \\ & \cdot [2\theta_0 Ra + (Nc(1-\tilde{\epsilon}) + Nr)]^2 + 6\theta_0 Ra[\theta_0 Ra + (Nc(1-\tilde{\epsilon}) + Nr)] \end{aligned} \right\} \frac{X^8}{8!} + \dots
 \end{aligned} \quad (51)$$

The values of the thermogeometric parameter, θ_0 are determined from Equations (50) and (51) using the Newton–Raphson iterative method.

4. Fin Efficiency

As established from previous works, the instantaneous total surface heat loss is the sum of the convective and radiative losses together with heat loss due to porosity and is expressed in Equation (41) as:

$$Q_{actual} = \int_0^L \left[hP(1-\tilde{\epsilon})(T - T_\infty) + \frac{\rho c_p g K \beta P}{v} (T - T_a)^2 + \sigma \epsilon P(T^4 - T_s^4) \right] dx \quad (52)$$

The ideal fin heat transfer is the heat transfer from the fin when the entire fin surface operates at the fin base temperature. Thus, the idea heat transfer from the fin is given as:

$$Q_{ideal} = hPL(1-\tilde{\epsilon})(T_b - T_\infty) + \frac{\rho c_p g K \beta P}{v} (T_b - T_a)^2 + \sigma \epsilon PL(T_b^4 - T_s^4) \quad (53)$$

Therefore, fin efficiency η could be expressed as the ratio of the actual rate of heat transfer of the fin to the rate that would be if the entire fin is at base temperature expressed as:

$$\eta = \frac{Q_f}{Q_{max}} = \frac{\int_0^L \left[hP(1-\tilde{\epsilon})(T - T_\infty) + \frac{\rho c_p g K \beta P}{v} (T - T_a)^2 + \sigma \epsilon P(T^4 - T_s^4) \right] dx}{hPL(1-\tilde{\epsilon})(T_b - T_\infty) + \frac{\rho c_p g K \beta P}{v} (T_b - T_a)^2 + \sigma \epsilon PL(T_b^4 - T_s^4)} \quad (54)$$

The dimensionless form of Equation (30) is given in Equation (31):

$$\eta = \frac{\int_0^1 \left\{ M_c^2 \theta + S_h \theta^2 + Nr_c \left[(\theta + C_T)^4 - C_T^4 \right] \right\} dX}{M_c^2 + S_h + Nr_c \left[(1 + C_T)^4 - C_T^4 \right]} \quad (55)$$

5. Results

The results of ADM for the comparison of the porous fin of homogeneous material (HM) and porous fin of FGM are presented in Figures 2–6. The figures highlight the effects of various thermal parameters of the fin.

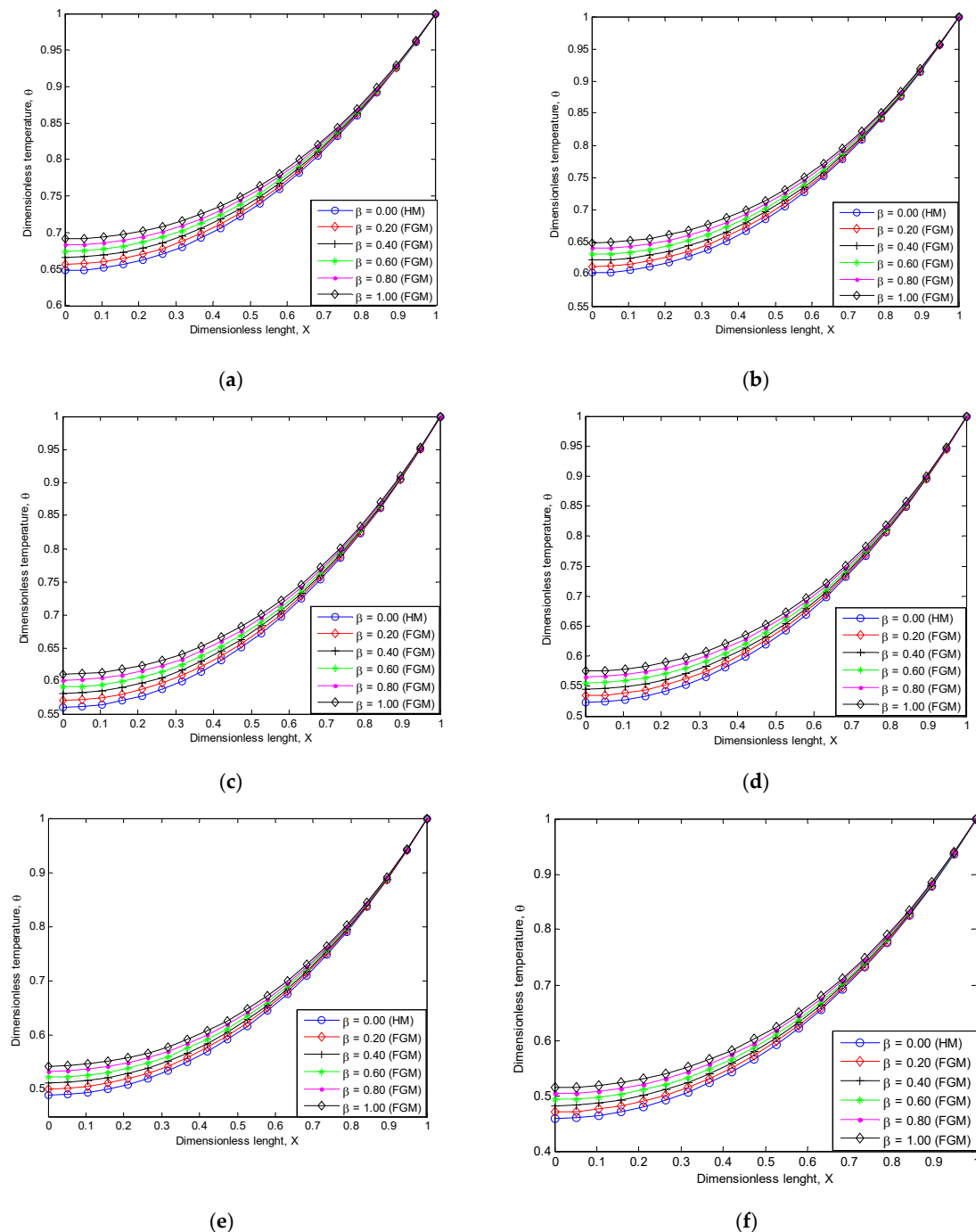


Figure 2. Fin dimensionless temperature profile for varying thermo-geometric parameter under linear-law function when: (a) $Nr = 0.0$, $Ra = 0.01$, $Nc = 1.0$; (b) $Nr = 0.2$, $Ra = 0.01$, $Nc = 1.0$; (c) $Nr = 0.1$, $Rd = 0.01$, $Nc = 1.0$; (d) $Nr = 0.1$, $Ra = 0.01$, $Nc = 1.2$; (e) $Nr = 0.1$, $Ra = 0.01$, $Nc = 1.5$; and (f) $Nr = 0.2$, $Ra = 0.01$, $Nc = 1.2$.

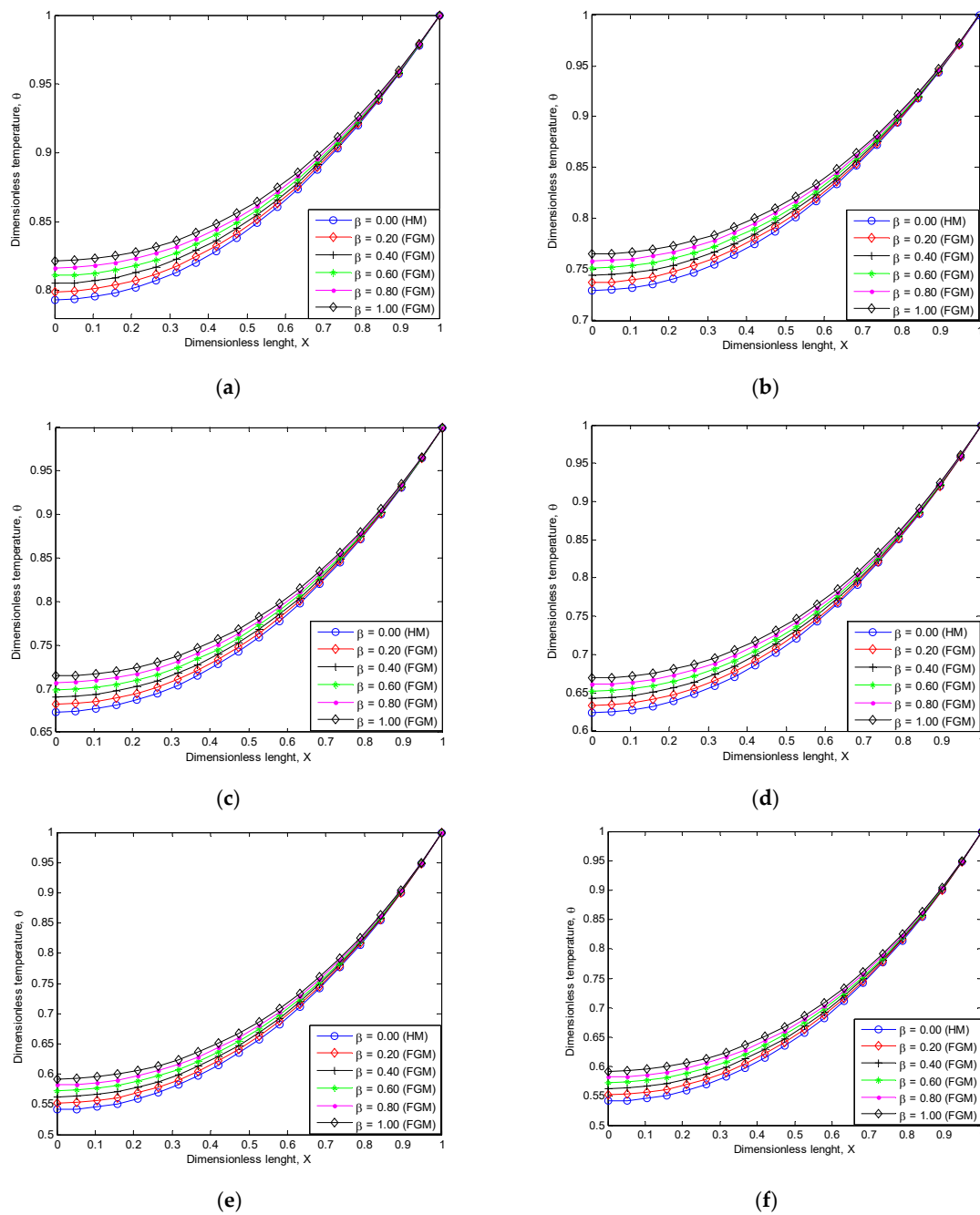


Figure 3. Fin dimensionless temperature profile for varying thermo-geometric parameter under linear-law function when: (a) $Nc = 0.5$, $Ra = 0.01$, $Nr = 0.0$; (b) $Nc = 0.1$, $Ra = 0.01$, $Nr = 0.2$; (c) $Nc = 0.1$, $Ra = 0.01$, $Nr = 0.4$; (d) $Nc = 0.2$, $Ra = 0.01$, $Nr = 0.3$; (e) $Nc = 0.5$, $Ra = 0.01$, $Nr = 0.2$; and (f) $Nr = 0.2$, $Ra = 0.01$, $Nr = 1.0$.

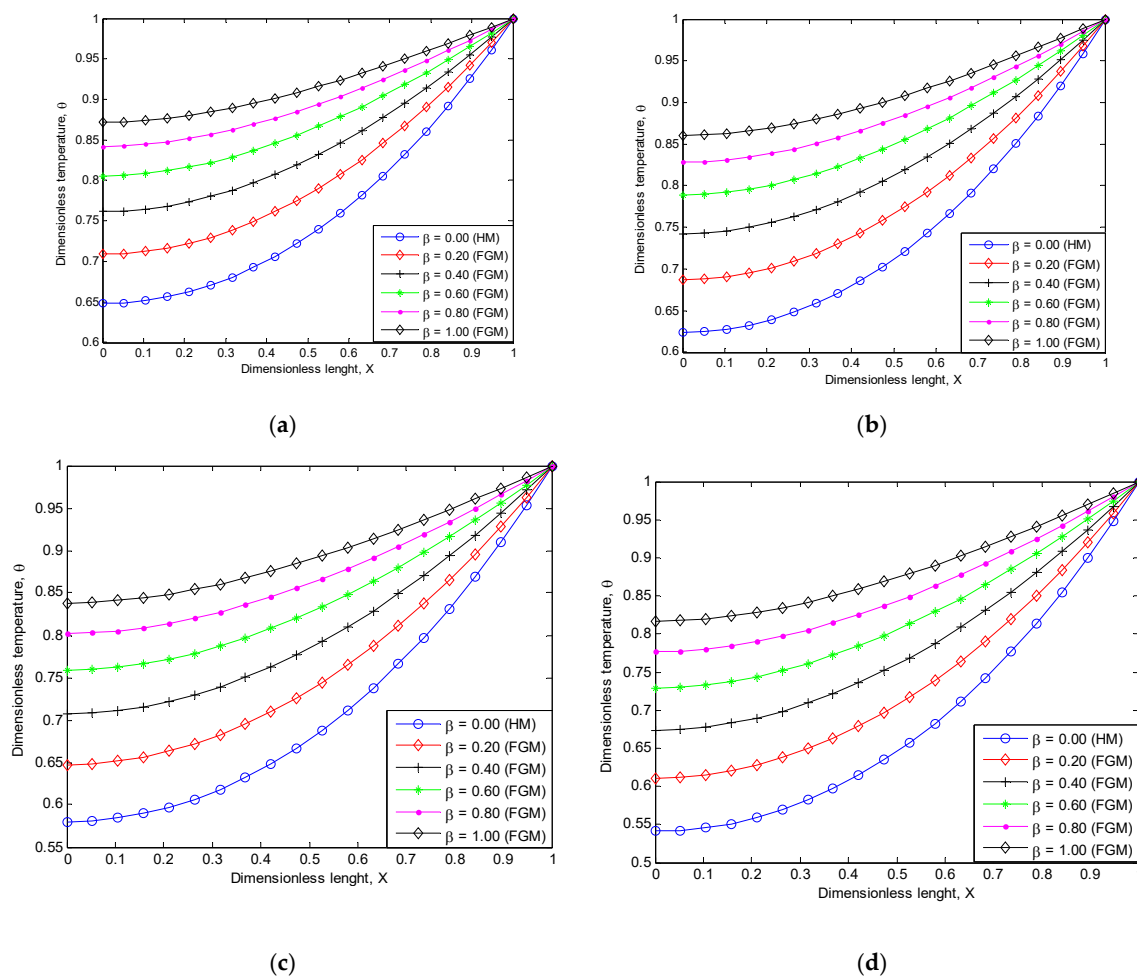


Figure 4. Fin dimensionless temperature profile for varying thermo-geometric parameter under power-law function when: (a) $Nr = 0.0$, $Ra = 0.01$, $Nc = 1.0$; (b) $Nr = 0.1$, $Ra = 0.01$, $Nc = 0.5$; (c) $Nr = 0.1$, $Ra = 0.01$, $Nc = 0.6$; and (d) $Nr = 0.2$, $Ra = 0.01$, $Nc = 0.5$.

Figures 2–4 shows the effect of the inhomogeneity index on the dimensionless temperature profile and heat transfer rate of the fin. Figure 2 highlights the results of the linear-law function, whilst Figures 3 and 4 highlight the results of the power law function. From the parametric result presented in Figures 2–4, it is seen that an increase in the inhomogeneity index improves the rate of heat transfer through the fin. The figures also show that for all values of the convective and radiative parameters, the temperature gradient along the fin with FGM was smaller than with fin of homogeneous material for both linear and power-law function. The inhomogeneity index β increases as the fin temperature gradient decreases, whilst the rate of heat transfer of longitudinal FGM fin increases as β increases. The results show that the temperature profiles of the FGM fin are highly sensitive in the power-law function compared to the linear-law function. Furthermore, it can be seen that the application of FGM is reliable at low thermogeometric, convective and radiative parameters since the difference in temperature profile between FGM fin and HM fin slightly decreases as the dimensionless thermogeometric parameter increases. Therefore, the application of fin of FGM decreases the thermal resistance along the fin such that FGM fin has a higher temperature at the fin tip than HM fin.

Figure 5 shows the effects of porosity on the fin's temperature profile, whereas Figure 6 highlights the effects of porosity on the thermal efficiency of the fin. From Figures 5 and 6, it is can be seen that increase in the porosity parameter causes the fin temperature to decrease rapidly, whilst the heat transfer rate through the fin increases as the fin temperature decreases faster. The rapid decrease in fin temperature is a result of an increase in the porosity parameter. This is due to the fact that as the fin

porosity increases, the permeability of the fin increases, which affects the ability of the working fluid to penetrate through fin pores to increase. The increased penetration of the working fluid increases the effect of the buoyancy force, which causes heat flow by convection to increase. Consequently, the increased rate of heat transfer by convection invariably improves the thermal performance of the fin as shown in Figure 7. Practically, the findings of the present study are useful among others for effective determination of coolant flow rate, which is essential in the designing miniaturized heatsinks with smaller volume fan for low energy consumption.

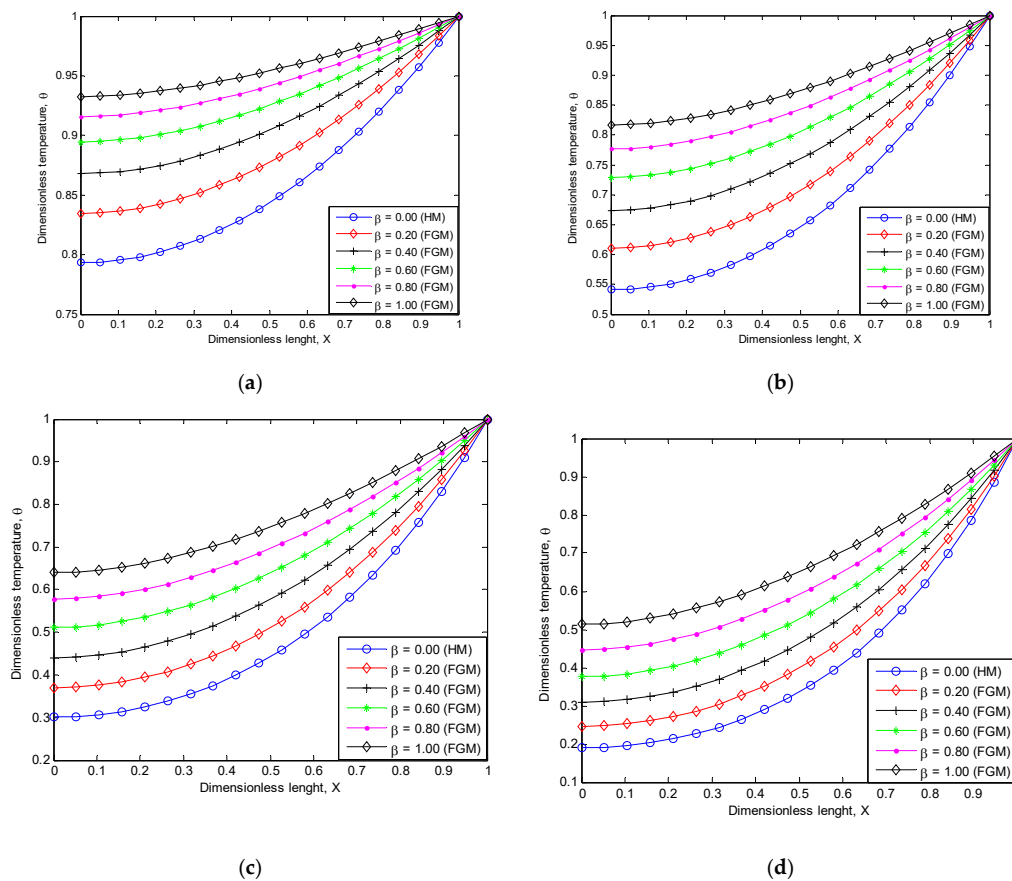


Figure 5. Fin dimensionless temperature profile for varying thermo-geometric parameter under power-law function when: (a) $Nc = 0.0$, $Ra = 0.01$, $Nr = 0.5$; (b) $Nc = 0.1$, $Ra = 0.01$, $Nr = 0.6$; (c) $Nc = 1.0$, $Ra = 0.01$, $Nr = 0.1$; and (d) $Nc = 2.0$, $Ra = 0.01$, $Nr = 0.2$.

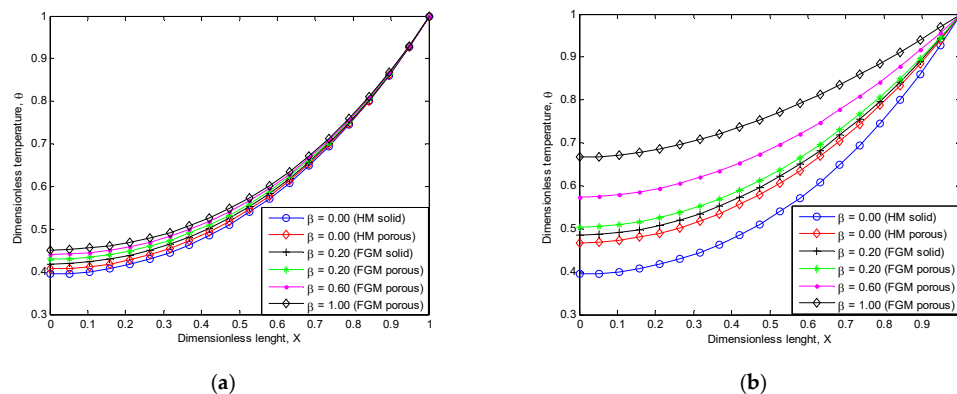


Figure 6. Fin dimensionless temperature profile for the varying thermogeometric parameter: (a) linear-law function and (b) power-law function.

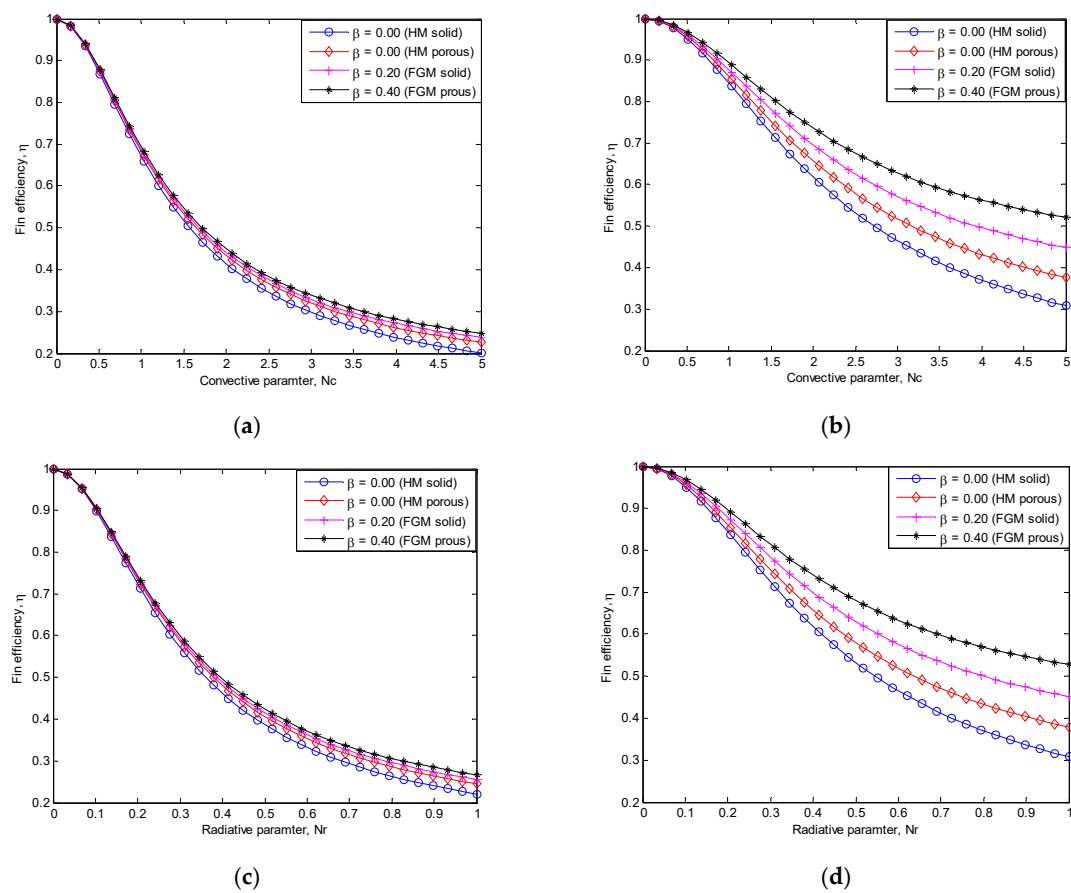


Figure 7. Fin efficiency for the varying thermo-geometric parameter: (a) linear-law function when $Nc = 1.0$, $Ra = 0.01$, $Nr = 0.1$; (b) power-law function $Nc = 1.0$, $Ra = 0.01$, $Nr = 0.2$; (c) linear-law function $Nc = 2.0$, $Ra = 0.01$, $Nr = 0.1$; and (d) power-law function $Nc = 2.0$, $Ra = 0.01$, $Nr = 0.1$.

Results from the present study were compared to other work as presented in Table 1. From Table 1 it is shown that the temperature result of ADM is reliable for temperature prediction of heatsinks as it agrees with numerical and ADM results.

Table 1. Comparison of temperature result.

X	Numerical Method (NM)	Homotopy Perturbation Method (HPM) [29]	Galerkin's Method of Weighted Residual (GMWR) [29]	Adomian Decomposition Method (ADM) (Present Study)	Absolute Error in HPM (NM-HPM)	Absolute Error in GMWR (NM-HPM)	Absolute Error in ADM (NM-HPM)
0.0	0.9581	0.9581	0.9581	0.9581	0.0000	0.0000	0.0000
0.1	0.9585	0.9585	0.9585	0.9585	0.0000	0.0000	0.0000
0.2	0.9597	0.9597	0.9597	0.9597	0.0000	0.0000	0.0000
0.3	0.9618	0.9618	0.9618	0.9618	0.0000	0.0000	0.0000
0.4	0.9647	0.9647	0.9647	0.9647	0.0000	0.0000	0.0000
0.5	0.9685	0.9685	0.9685	0.9685	0.0000	0.0000	0.0000
0.6	0.9730	0.9730	0.9730	0.9730	0.0000	0.0000	0.0000
0.7	0.9785	0.9785	0.9785	0.9785	0.0000	0.0000	0.0000
0.8	0.9846	0.9846	0.9846	0.9846	0.0000	0.0000	0.0000
0.9	0.9919	0.9919	0.9919	0.9919	0.0000	0.0000	0.0000
1.0	1.0000	1.0000	1.0000	1.0000	0.0000	0.0000	0.0000

6. Conclusions

We have carried out a thermal investigation on the performance of a porous fin heatsink of FGM for reliable thermal prediction. We solve the developed thermal models via the Adomian decomposition method and investigate the effects of inhomogeneity index of FGM and thermo-geometric parameter on the thermal performance of the porous fin heatsink. The parametric study shows that increase in the inhomogeneity index of FGM, convective and radiative parameter improves the thermal efficiency of the porous fin heatsink. It is also shown that the temperature profile of the FGM fin is highly sensitive in power-law function compared to the linear-law function. Furthermore, the application of fin of FGM decreases the thermal resistance along the fin such that FGM fin has a higher temperature at the fin tip compared with HM fin. The viability of FGM in heatsink design to achieve improved cooling in comparison with conventional HM heatsink is highlighted. The findings of the present study are of practical implications to achieve thermally-enhanced heatsinks of FGM for improved cooling of electronic systems.

Author Contributions: Conceptualization, G.O. Methodology, G.O. and G.S.; Formal Analysis, G.O. and G.S.; Validation, Y.A.; Writing Original Draft Preparation, G.O. and Y.A.; Review and Editing, G.O. and G.S.; Supervision, R.A.

Funding: This research received no external funding and the APC was funded by the first author.

Acknowledgments: The first author wishes to express his gratitude for the sponsorship by the Tertiary Education Trust Fund (TETFund) of Federal Government of Nigeria.

Conflicts of Interest: The authors declare no conflict of interest.

Nomenclature

A	Fin cross-sectional area, m^2
P	Fin perimeter, m
h_b	Heat transfer coefficient at the base of the fin, $Wm^{-2}K^{-1}$
c_p	Specific heat of the fluid passing through porous fin, $J/kg\cdot K$
h	Heat transfer coefficient over the fin surface, W/m^2K
H	Dimensionless heat transfer coefficient at fin base, $Wm^{-2}K^{-1}$
k	Thermal conductivity of fin material, $Wm^{-1}K^{-1}$
k_b	Thermal conductivity of fin material at fin base, $Wm^{-1}K^{-1}$
k_{eff}	Effective thermal conductivity ratio
K	Permeability
T	Fin temperature, K
T_b	Base temperature, K
T_a	Ambient temperature, K
X	Dimensionless fin length
g	Gravity constant m/s^2
Da	Darcy number
Ra	Rayleigh number
S_h	Porosity parameter
Nc	Convective heat parameter
Nr	Radiative heat parameter
M	Dimensionless thermo-geometric parameter

Greek Symbols

δ	Fin thickness, m
δ_b	Fin base thickness
β	inhomogeneity index
θ_b	Dimensionless temperature at fin base
ε	Pores parameter
ϕ	Porosity or void ratio
η	Fin efficiency
ν	kinematic viscosity, m^2/s
ρ	Density of the fluid, kg/m^3
σ	Stefan-Boltzmann constant

References

1. Kiwan, S.; Al-Nimr, M.A. Using Porous Fins for Heat Transfer Enhancement. *J. Heat Transf.* **2000**, *123*, 790–795. [\[CrossRef\]](#)
2. Das, R.; Kundu, B. Prediction of Heat Generation in a Porous Fin from Surface Temperature. *J. Thermophys. Heat Transf.* **2017**, *31*, 781–790. [\[CrossRef\]](#)
3. Oguntala, G.; Sobamowo, G.; Ahmed, Y.; Abd-Alhameed, R. Application of Approximate Analytical Technique Using the Homotopy Perturbation Method to Study the Inclination Effect on the Thermal Behavior of Porous Fin Heat Sink. *Math. Comput. Appl.* **2018**, *23*, 62. [\[CrossRef\]](#)
4. Torabi, M.; Aziz, A.; Zhang, K. A comparative study of longitudinal fins of rectangular, trapezoidal and concave parabolic profiles with multiple nonlinearities. *Energy* **2013**, *51*, 243–256. [\[CrossRef\]](#)
5. Kundu, B.; Das, R.; Wankhade, A.; Lee, K.-S. Heat transfer improvement of a wet fin under transient response with a unique design arrangement aspect. *Int. J. Heat Mass Transf.* **2018**, *127*, 1239–1251. [\[CrossRef\]](#)
6. Kundu, B.; Wongwises, S. A decomposition analysis on convecting–radiating rectangular plate fins for variable thermal conductivity and heat transfer coefficient. *J. Frankl. Inst.* **2012**, *349*, 966–984. [\[CrossRef\]](#)
7. Oguntala, G.; Abd-Alhameed, R. Thermal Analysis of Convective-Radiative Fin with Temperature-Dependent Thermal Conductivity Using Chebychev Spectral Collocation Method. *J. Appl. Comput. Mech.* **2018**, *4*, 87–94.
8. Oguntala, G.; Abd-Alhameed, R.; Sobamowo, G.; Danjuma, I. Performance, Thermal Stability and Optimum Design Analyses of Rectangular Fin with Temperature-Dependent Thermal Properties and Internal Heat Generation. *J. Comput. Appl. Mech.* **2018**, *49*, 37–43.
9. Kundu, B.; Bhanja, D.; Lee, K.-S. A model on the basis of analytics for computing maximum heat transfer in porous fins. *Int. J. Heat Mass Transf.* **2012**, *55*, 7611–7622. [\[CrossRef\]](#)
10. Singh, K.; Das, R.; Kundu, B. Approximate Analytical Method for Porous Stepped Fins with Temperature-Dependent Heat Transfer Parameters. *J. Thermophys. Heat Transf.* **2016**, *30*, 661–672. [\[CrossRef\]](#)
11. Das, R. Forward and inverse solutions of a conductive, convective and radiative cylindrical porous fin. *Energy Convers. Manag.* **2014**, *87*, 96–106. [\[CrossRef\]](#)
12. Oguntala, G.; Sobamowo, G.; Abd-Alhameed, R.; Jones, S. Efficient Iterative Method for Investigation of Convective–Radiative Porous Fin with Internal Heat Generation Under a Uniform Magnetic Field. *Int. J. Appl. Comput. Math.* **2019**, *5*, 13. [\[CrossRef\]](#)
13. Oguntala, G.A.; Sobamowo, M.G. Galerkin’s Method of Weighted Residual for a Convective Straight Fin with Temperature-Dependent Conductivity and Internal Heat Generation. *Int. J. Eng. Technol.* **2016**, *6*, 432–442.
14. Oguntala, G.; Sobamowo, G.; Abd-Alhameed, R. Numerical analysis of transient response of convective-radiative cooling fin with convective tip under magnetic field for reliable thermal management of electronic systems. *Therm. Sci. Eng. Prog.* **2019**, *9*, 289–298. [\[CrossRef\]](#)
15. Oguntala, G.A.; Abd-Alhameed, R.A. Haar Wavelet Collocation Method for Thermal Analysis of Porous Fin with Temperature-dependent Thermal Conductivity and Internal Heat Generation. *J. Appl. Comput. Mech.* **2017**, *3*, 185–191.
16. Das, R.; Kundu, B. Direct and inverse approaches for analysis and optimization of fins under sensible and latent heat load. *Int. J. Heat Mass Transf.* **2018**, *124*, 331–343. [\[CrossRef\]](#)
17. Seyf, H.R.; Feizbakhshi, M. Computational analysis of nanofluid effects on convective heat transfer enhancement of micro-pin-fin heat sinks. *Int. J. Therm. Sci.* **2012**, *58*, 168–179. [\[CrossRef\]](#)
18. Fazeli, S.A.; Hashemi, H.; Mohammad, S.; Zirakzadeh, H.; Ashjaee, M. Experimental and numerical investigation of heat transfer in a miniature heat sink utilizing silica nanofluid. *Superlattices Microstruct.* **2012**, *51*, 247–264. [\[CrossRef\]](#)
19. Kim, S.-M.; Mudawar, I. Analytical heat diffusion models for different micro-channel heat sink cross-sectional geometries. *Int. J. Heat Mass Transf.* **2010**, *53*, 4002–4016. [\[CrossRef\]](#)
20. Naphon, P.; Klangchart, S.; Wongwises, S. Numerical investigation on the heat transfer and flow in the mini-fin heat sink for CPU. *Int. Commun. Heat Mass Transf.* **2009**, *36*, 834–840. [\[CrossRef\]](#)
21. Naphon, P.; Khonseur, O. Study on the convective heat transfer and pressure drop in the micro-channel heat sink. *Int. Commun. Heat Mass Transf.* **2009**, *36*, 39–44. [\[CrossRef\]](#)

22. Kim, T.Y.; Kim, S.J. Fluid flow and heat transfer characteristics of cross-cut heat sinks. *Int. J. Heat Mass Transf.* **2009**, *52*, 5358–5370. [[CrossRef](#)]
23. Oguntala, G.A.; Abd-Alhameed, R.A.; Sobamowo, G.M.; Eya, N. Effects of particles deposition on thermal performance of a convective-radiative heat sink porous fin of an electronic component. *Therm. Sci. Eng. Prog.* **2018**, *6*, 177–185. [[CrossRef](#)]
24. Oguntala, G.; Abd-Alhameed, R. Performance of convective-radiative porous fin heat sink under the influence of particle deposition and adhesion for thermal enhancement of electronic components. *Karbala Int. J. Mod. Sci.* **2018**, *4*, 297–312. [[CrossRef](#)]
25. Oguntala, G.A.; Sobamowo, G.M.; Eya, N.N.; Abd-Alhameed, R.A. Investigation of Simultaneous Effects of Surface Roughness, Porosity, and Magnetic Field of Rough Porous Microfin Under a Convective–Radiative Heat Transfer for Improved Microprocessor Cooling of Consumer Electronics. *IEEE Trans. Compon. Packag. Manuf. Technol.* **2019**, *9*, 235–246. [[CrossRef](#)]
26. Wan, Z.M.; Guo, G.Q.; Su, K.L.; Tu, Z.K.; Liu, W. Experimental analysis of flow and heat transfer in a miniature porous heat sink for high heat flux application. *Int. J. Heat Mass Transf.* **2012**, *55*, 4437–4441. [[CrossRef](#)]
27. Oguntala, G.; Abd-Alhameed, R.; Sobamowo, G. On the effect of magnetic field on thermal performance of convective-radiative fin with temperature-dependent thermal conductivity. *Karbala Int. J. Mod. Sci.* **2018**, *4*, 1–11. [[CrossRef](#)]
28. Sobamowo, M.G.; Oguntala, G.A.; Yinusa, A.A. Nonlinear Transient Thermal Modeling and Analysis of a Convective-Radiative Fin with Functionally Graded Material in a Magnetic Environment. *Model. Simul. Eng.* **2019**, *2019*, 7878564. [[CrossRef](#)]
29. Sobamowo, M.G.; Kamiyo, O.M.; Adeleye, O.A. Thermal performance analysis of a natural convection porous fin with temperature-dependent thermal conductivity and internal heat generation. *Therm. Sci. Eng. Prog.* **2017**, *1*, 39–52. [[CrossRef](#)]



© 2019 by the authors. Licensee MDPI, Basel, Switzerland. This article is an open access article distributed under the terms and conditions of the Creative Commons Attribution (CC BY) license (<http://creativecommons.org/licenses/by/4.0/>).